

SILVER ISOTOPIC EVIDENCE FOR IMPACT-DRIVEN VOLATILE LOSS FROM DIFFERENTIATED ASTEROIDS. T. Kleine¹, M. Matthes¹, F. Nimmo² and I. Leya³, ¹Institut für Planetologie, University of Münster, 48149 Münster, Germany (thorsten.kleine@wwu.de), ²Dep. Earth & Planet. Sci., University of California Santa Cruz, Santa Cruz, CA 95064, USA, ³Space Research and Planetology, University of Bern, Bern, Switzerland.

Introduction: Terrestrial planets and most differentiated asteroids are depleted in volatile elements compared to primitive chondrites and the bulk solar system. However, the origin of these volatile depletions and whether they result from processes associated with planetary accretion or from prior fractionations in the solar nebula are unclear.

Group IVB irons are among the most strongly volatile-depleted meteorites [1,2], making them ideal targets for investigating the process of volatile depletion. Recent work, utilizing nucleosynthetic isotope anomalies as genetic tracers, has shown that the IVB irons belong to the carbonaceous suite of meteorites [3]. These likely formed beyond the orbit of Jupiter [4], implying that the IVB parent body accreted beyond the ice line and, hence, was volatile-rich initially. This raises the question of when and how the IVB irons lost their volatiles. Addressing this question is important not only for understanding the evolution of volatile-poor differentiated asteroids, but also to more generally constrain the process of volatile depletion and, ultimately, volatile accretion to the terrestrial planets.

To address these issues, we applied the short-lived ^{107}Pd - ^{107}Ag system to IVB irons. This system is ideally suited to date iron meteorites [5], and, as Ag is strongly volatile, also to determine the timescale of volatile fractionation [6]. Although the IVB irons were among the first irons for which Pd-Ag data were reported [7], until now there has been no study investigating the Pd-Ag chronology of volatile depletion in the IVB irons.

Methods: Nine different metal pieces (~5–10 g) of the IVB iron Dumont were selected for this study. The chemical separation of Ag and the measurement of Ag isotopic compositions and Pd/Ag ratios followed our established procedures using the Neptune *Plus* MC-ICPMS at Münster [8,9]. As the IVB irons are extremely depleted in Ag, reliable Pd-Ag measurements for these irons require low and reproducible blanks. During this study, total procedural blanks were <20 pg Ag, resulting in blank corrections on $^{107}\text{Ag}/^{109}\text{Ag}$ of ~1–2%, much smaller than the ~26% total variation observed among the investigated samples. Finally, to quantify Ag isotope shifts induced by the interaction with galactic cosmic rays (GCR), Pt isotopic compositions were also measured for each sample [9].

Results: The Dumont samples display correlated variations in $^{108}\text{Pd}/^{109}\text{Ag}$ and $^{107}\text{Ag}/^{109}\text{Ag}$ (Fig. 1). The same samples also exhibit Pt isotope anomalies ($\epsilon^{196}\text{Pt}$

~0.4), indicating substantial GCR-induced neutron capture effects. The dominant GCR-induced reaction is $^{108}\text{Pd}(n,\gamma)^{109}\text{Pd}(\beta^-)^{109}\text{Ag}$, and so for samples with very high $^{108}\text{Pd}/^{109}\text{Ag}$, such as the IVB irons, both the $^{107}\text{Ag}/^{109}\text{Ag}$ and $^{108}\text{Pd}/^{109}\text{Ag}$ are affected. As the GCR shifts on $^{107}\text{Ag}/^{109}\text{Ag}$ depend on $^{108}\text{Pd}/^{109}\text{Ag}$, both values have to be corrected iteratively. This correction results in substantially more radiogenic $^{107}\text{Ag}/^{109}\text{Ag}$ and correlated high $^{108}\text{Pd}/^{109}\text{Ag}$ (Fig. 1).

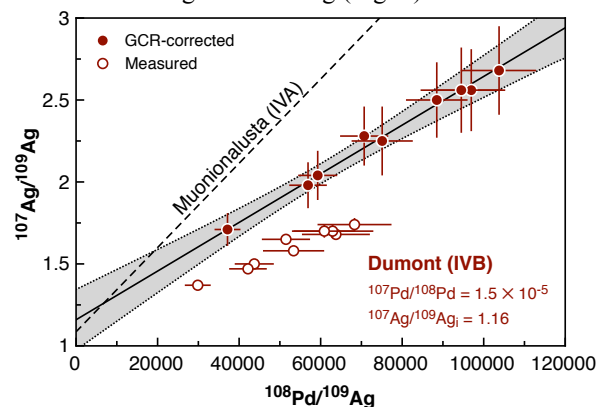


Fig. 1: Pd-Ag isochron for the IVB iron Dumont. Isochron for the IVA iron Muonionalusta shown for comparison.

Pd-Ag systematics: The GCR-corrected Pd-Ag data for different samples from Dumont plot on a single Pd-Ag isochron, whose slope corresponds to an initial $^{107}\text{Pd}/^{108}\text{Pd}$ of $\sim 1.5 \times 10^{-5}$ (Fig. 1). This is the lowest initial $^{107}\text{Pd}/^{108}\text{Pd}$ yet reported for iron meteorites; for instance, the IVA iron Muonionalusta has an initial $^{107}\text{Pd}/^{108}\text{Pd}$ of $(2.57 \pm 0.07) \times 10^{-5}$ [6,8], indicating that the IVB core cooled below Pd-Ag closure ~5 Ma later than the IVA core (Fig. 1). Current estimates of the solar system initial $^{107}\text{Pd}/^{108}\text{Pd}$ range between $\sim 3.5 \times 10^{-5}$ and $\sim 6.6 \times 10^{-5}$ [8], indicating that the IVB core cooled below Pd-Ag closure between ~8 and ~14 Ma after solar system formation. In spite of this late Pd-Ag closure and the exceedingly high $^{108}\text{Pd}/^{109}\text{Ag}$ of the IVB irons, the initial $^{107}\text{Ag}/^{109}\text{Ag}$ of the Dumont isochron is not significantly elevated and overlaps with the chondritic Ag isotopic composition [10] (Fig. 2).

Ag isotopic evolution of the IVB core: The initial $^{107}\text{Ag}/^{109}\text{Ag}$ of Dumont may be compared to the expected Ag isotopic evolution of the IVB core, calculated using the bulk $^{108}\text{Pd}/^{109}\text{Ag}$ of the core as inferred from fractional crystallization modeling. We used the same model as in previous studies on IVA irons [6,8], and assumed a S content of 1 wt.% and a Pd concentra-

tion of 8.6 ppm for the bulk core [2]. The modeling shows that the ^{109}Ag content of the bulk core must have been lower than ~ 30 ppt, because otherwise the most ^{109}Ag -depleted metal sample from Dumont would plot outside the field between the calculated solid and liquid evolution tracks. Using this value results in $^{108}\text{Pd}/^{109}\text{Ag} \approx 76,000$ for the bulk IVB core.

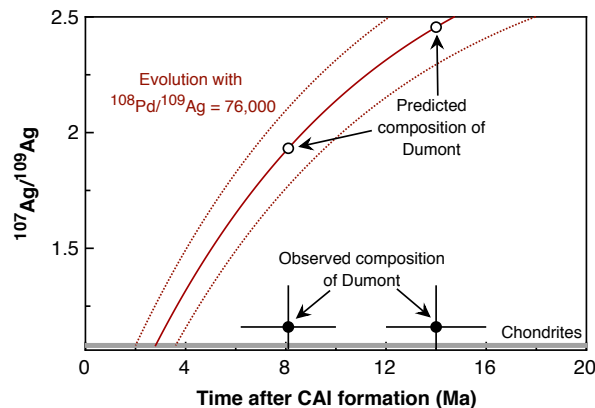


Fig. 2: Predicted Ag isotopic evolution of the IVB core, starting at the time of core formation of 2.8 ± 0.8 Ma (solid line shows evolution starting at 2.8 Ma, dotted lines at 0.8 Ma earlier and later). Note the much lower initial $^{107}\text{Ag}/^{109}\text{Ag}$ observed for the IVB iron Dumont. The near-horizontal gray line represents the Ag isotopic evolution of chondrites.

Hf-W systematics indicate that the IVB core formed at 2.8 ± 0.8 Ma after CAI formation [11], ~ 5 – 11 Ma before cooling below Pd-Ag closure. Thus, if the high $^{108}\text{Pd}/^{109}\text{Ag}$ of the IVB core were established at the time of core formation, then the initial $^{107}\text{Ag}/^{109}\text{Ag}$ of Dumont at the time of Pd-Ag closure would have been between ~ 1.9 and ~ 2.4 (Fig. 2). The much lower initial $^{107}\text{Ag}/^{109}\text{Ag} \approx 1.16$ of Dumont, therefore, indicates that prior to cooling and crystallization, the IVB core must have evolved with a much lower $^{108}\text{Pd}/^{109}\text{Ag}$. Consequently, there must have been a late Pd-Ag fractionation (i.e., Ag loss) in the IVB core, postdating core formation by at least ~ 5 Ma (Fig. 2). Moreover, once the $^{108}\text{Pd}/^{109}\text{Ag}$ of $\sim 76,000$ of the IVB core had been established, the initial $^{107}\text{Ag}/^{109}\text{Ag}$ of Dumont was reached within < 2 Ma (Fig. 2), indicating that subsequent to the late Pd-Ag fractionation, crystallization and cooling of the IVB core occurred very rapidly.

Impact-driven volatile loss from the IVB parent body: As a chalcophile and strongly volatile element, significant Ag loss from the IVB core can occur by separation of either a S-rich melt or a vapour phase. The segregation of a S-rich melt would have mainly affected Ag but not other volatile, less chalcophile elements (e.g., Ge) [8]. However, as the IVB parent body presumably formed beyond the ice line [3,4], it must have been volatile-rich initially, implying that not only Ag but also other volatile elements were lost at a

later stage. Thus, the late Pd-Ag fractionation in the IVB core most likely results from volatile loss, removing Ag and other volatiles from the core.

Loss of volatiles from a metallic core is most likely if the core was exposed to space and was still molten. Thermal models for differentiated asteroids reveal that the cores of 100–200 km-sized bodies (the size of the IVB body inferred from metallographic cooling rates [12]) would still be liquid at the time given by the Pd-Ag age of Dumont. Thus, impact disruption of the progenitor to the IVB parent body, resulting in stripping of the mantle [12], would have exposed a still-molten metallic body. The exposure would have also facilitated rapid cooling and crystallization, as mandated by the Pd-Ag data. A corollary of this is that the Pd-Ag age most likely provides the time of impact disruption.

One possible pathway to volatile loss is pressure release (through removal of the overlying mantle), which in turn reduces the solubilities of volatile species in the metallic magma and promotes degassing. Of note, this process does not necessarily induce a large kinetic isotope fractionation (unlike evaporation from the surface), because the gas likely equilibrated with the surrounding metallic magma during its ascent to the surface. An alternative possibility is removal of volatiles via reaction with oxidized mantle material during the catastrophic disruption event.

Conclusions: The Pd-Ag isotope systematics of the IVB iron Dumont strongly suggest that the extreme volatile element depletion of at least some differentiated asteroids result from catastrophic disruption. In the case of the IVB irons this process occurred relatively late, ~ 8 – 14 Ma after solar system formation. This timescale coincides with the predicted time of enhanced collisions related to the growth and/or migration of the gas giants, during which carbonaceous-type bodies were scattered into the inner solar system [4,13]. While this scattering process will have delivered volatiles to the inner solar system, in some cases (like the IVB irons) it rather resulted in volatile loss.

References: [1] Campbell A.J. and Humayun M. (2005) *GCA*, 69, 4733–4744. [2] Walker R.J. et al. (2008) *GCA*, 72, 2198–2216. [3] Budde G. et al. (2016) *EPSL*, 454, 293–303. [4] Kruijjer T.S. et al. (2017) *PNAS*, 114, 6712–6716. [5] Chen J.H. and Wasserburg G.J. (1990) *GCA*, 54, 1729–1743. [6] Horan M.F. et al. (2012) *EPSL*, 351, 215–222. [7] Kelly W.R. and Wasserburg G.J. (1978) *GRL*, 5, 1079–1082. [8] Matthes M. et al. (2018) *GCA*, 220, 82–95. [9] Matthes M. et al. (2015) *GCA*, 169, 45–62. [10] Schönbacher M. et al. (2008) *GCA*, 72, 5330–5341. [11] Kruijjer T.S. et al. (2014) *Science*, 344, 1150–1154. [12] Yang J. et al. (2010) *GCA*, 74, 4493–4506. [13] Walsh K.J. et al. (2011) *Nature*, 475, 206–209.